Wave packet driven dissociation and concerted elimination in CH_2I_2

Dominik Geißler, Brett J. Pearson,[a] and Thomas Weinacht[b]
Department of Physics, Stony Brook University, Stony Brook, New York 11794, USA

(Received 11 September 2007; accepted 11 October 2007; published online 27 November 2007)

We follow the evolution of a vibrational wave packet in a highly excited state of the halogenated methane CH_2I_2. We observe how the wave packet modulates both dissociation and concerted elimination to form CH_2I^+ and I_2^+, respectively. We present a simple and intuitive interpretation of the molecular dynamics leading to the formation of the products. © *2007 American Institute of Physics*. [DOI: 10.1063/1.2805186]

I. INTRODUCTION

Vibrational wave packets play an important role in driving coherent chemistry and molecular imaging.[1–6] There is significant interest in extending wave packet measurements and controlled bond breaking from diatomic molecules to larger polyatomic systems.[7–10] Experiments and calculations aimed at observing and controlling dynamics in the halomethane family of molecules[11,12] have been motivated by their importance in atmospheric chemistry[13] and the fact that they serve as prototypes for laser controlled chemistry.[14] In addition to bond breaking, several experiments have used ultrafast lasers to drive and control concerted elimination in this family of molecules.[15–17]

Prior ultrafast laser measurements of I_2 and I_2^+ production from CH_2I_2 have demonstrated concerted elimination of the I_2 and I_2^+ products from the parent molecule.[17,18] Control over the I_2 yield has been demonstrated via laser pulse chirp,[19] and vibrational coherences have been observed in the I_2 product. Here, we present measurements where vibrational coherences in the reactant modulate the product yield. We show molecular dissociation and concerted elimination in CH_2I_2 driven by an ultrafast laser pulse and modulated by wave packet motion along one dimension of the full molecular potential energy surface. The picture that emerges is simple and intuitive.

II. THE EXPERIMENTAL APPARATUS

We begin with pulses from an amplified titanium:sapphire laser system (for a more detailed description of the experimental apparatus, see Ref. 20). The repetition rate, central wavelength, pulse duration, and pulse energy of the laser pulses are 1 kHz, 780 nm, 30 fs, and 1 mJ, respectively. The pulses from the amplifier system are directed into a Mach-Zehnder interferometer. One arm of the interferometer contains a pulse shaper with a computer-controlled, acousto-optic modulator (AOM) as the shaping element.[21] The interferometer with AOM allows us to vary both the pump-probe delay as well as the probe pulse shape. For the experiments described in this paper, we use the AOM only as a variable attenuator to change the probe pulse intensity. The two pulses are focused and intersect in an effusive molecular beam inside a vacuum chamber equipped with a time-of-flight mass spectrometer (TOFMS) that resolves the different fragment ions. TOFMS are recorded as a function of pump-probe delay and probe pulse intensity, resulting in a two-dimensional data set. All the data presented here were taken with a peak pump pulse intensity of 135 TW/cm^2.

III. RESULTS

Figure 1 shows the $CH_2I_2^+$, CH_2I^+, and I_2^+ fragments derived from CH_2I_2, as well as I_2^+ from a pure I_2 sample, as a function of pump-probe delay. As discussed above, we recorded the molecular fragment ion yields as a function of both pump-probe delay and probe pulse intensity. However, as the observed modulations in the fragment ion yields did not change over a range of probe pulse intensities (41 to 73 TW/cm^2), for the data shown in Fig. 1, we have integrated over this range of probe pulse intensities in order to maximize our signal to noise ratio. The pump-probe delay was varied from −500 to 4000 fs with a step size of 9.9 fs.

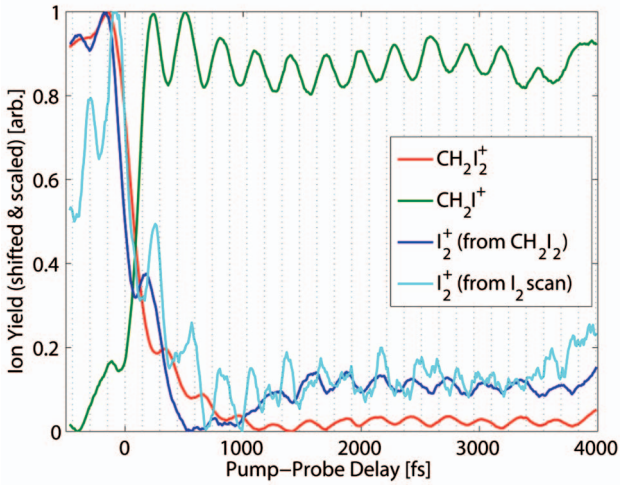

FIG. 1. (Color) Ion yields for several fragments as a function of pump-probe delay. They are individually scaled and shifted such that they are plotted between their minimum and maximum ion yields. The yields are averaged over probe intensities from 41 to 73 TW/cm^2. The dashed vertical lines have a spacing that corresponds to an oscillation frequency of 113 cm^{-1} [expected I–C–I scissors frequency in $CH_2I_2^+$ (Ref. 25)].

[a]Present Address: Department of Physics and Astronomy, Dickinson College, Carlisle, Pennsylvania 17013, USA.
[b]Electronic mail: thomas.weinacht@stonybrook.edu

 © 2007 American Institute of Physics

Downloaded 06 Dec 2007 to 129.49.60.83. Redistribution subject to AIP license or copyright; see http://jcp.aip.org/jcp/copyright.jsp

TABLE I. Maximum and minimum ion yields and oscillation amplitudes (in %, normalized to the maximum CH_2I^+ signal) for fragments from CH_2I_2 at a probe intensity of 73 TW/cm^2. The oscillation amplitudes have been averaged over positive pump-probe delays.

Fragment	Maximum yield	Minimum yield	Oscillation amplitude
$CH_2I_2^+$	66.5	29.5	0.92
CH_2I^+	100	89.1	1.10
I_2^+	11.0	8.17	0.12

Measurements were made using both a CH_2I_2 sample and a pure I_2 sample, in order to differentiate between laser driven concerted elimination and simply ionization of background I_2 in the interaction region.

As the data for each fragment ion are normalized to their maximum value, Table I lists the relative ion yields for comparison. Measurements of the fragment ion yields as a function of pump pulse intensity indicate that for the intensity of the pump pulse used in our experiments, the ionization of the sample is saturated.[23] For a fully ionized molecular sample, the I_2^+ yield ($\sim$0.06) is about an order of magnitude larger than the I_2 yield found for excitation of the molecule with continuous wave radiation at $\sim$9.4 eV.[22]

The yields for all three fragments from CH_2I_2 ($CH_2I_2^+$, CH_2I^+, and I_2^+) show modulations as a function of pump-probe delay with an identical frequency and a well-defined phase relationship. However, the modulation in I_2^+ derived from a pure I_2 sample is at a different frequency from the others and, therefore, not locked in phase. This is made more clear by Fourier transforming the full, two-dimensional data set along the time axis to provide a measure of the frequency content (inverse pump-probe delay, in wave numbers) as a function of probe pulse intensity. These data for all four fragments are shown in Fig. 2.

The $CH_2I_2^+$ [panel (b)] and CH_2I^+ fragments [panel (c)] both oscillate at 111 cm^{-1}, while the I_2^+ signal from the CH_2I_2 sample [panel (a)] shows Fourier components at both

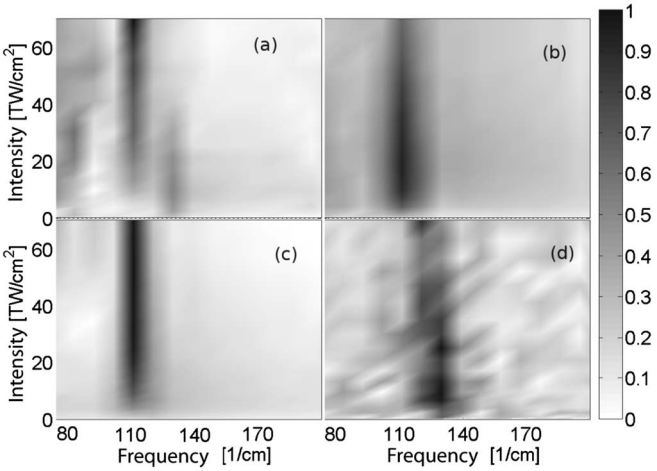

FIG. 2. Panels: (a) I_2^+ (from CH_2I_2), (b) $CH_2I_2^+$, (c) CH_2I^+, and (d) I_2^+ (from I_2). Plots show the Fourier transformation of the temporal pump-probe signals vs both frequency and probe intensity. The pump intensity was constant at 135 TW/cm^2, while probe intensity was varied from 0 to 73 TW/cm in 21 steps.

TABLE II. Frequencies of all vibrational modes involving at least one iodine atom in CH_2I_2, $CH_2I_2^+$, and iso-CH_2I_2 (taken from Refs. 25 and 28). All frequencies are given in wave numbers (cm^{-1}). Theoretical results are written in parentheses.

	Mode		
Molecule	I–C–I scissors	C–I_2 s.-str.	C–I_2 a.-str.
CH_2I_2	121[a] (127)	486 (486)	570 (568)
$CH_2I_2^+$	(113)	(537)	(503)

	Mode		
Molecule	C–I–I scissors	I–I stretch	C–I stretch
iso-CH_2I_2	110 (97)	128 (127)	701 (733)

[a]However, 127 cm^{-1} in Ref. 27.

111 and 130 cm^{-1}. At lower probe intensities, the I_2^+ signal from the pure iodine sample [panel (d)] is dominated by a similar component at 130 cm^{-1}. This contribution continually decreases in favor of an oscillation at 121 cm^{-1} as the probe intensity increases.

IV. DISCUSSION

The observed modulations in the fragment ion yields are a clear indication of vibrational wave packet dynamics. Here, we address what molecular motion leads to the modulations and how the various yields are related. As mentioned, an important first observation from the data is that the I_2^+ signal from the CH_2I_2 sample behaves differently from the I_2^+ signal from the I_2 sample. As the vibrational frequencies for many excited states of I_2 are known,[24] we can identify states in which wave packet dynamics modulate the I_2^+ yield. Specifically, we identify the modulation at 130 cm^{-1} with wave packet oscillations in the $A\,^4\Sigma_u^-$ state in excited I_2^+ [Ref. 24 gives a frequency of (128$\pm$2) cm^{-1} for this mode].

This means that for low probe intensities, the I_2^+ signal derived from CH_2I_2 appears to be dominated by wave packet oscillations in I_2^+ that modulate its dissociation into I^+, which is antiphased with the I_2^+ modulation at low probe intensity (not shown). More importantly, the 111 cm^{-1} component of the I_2^+ signal derived from CH_2I_2 has no counterpart in the measurements with pure iodine. We conclude that the oscillations at 111 cm^{-1} observed in I_2^+ above 6.5 TW/cm^2 probe intensity are due to I_2^+ formed coherently by the laser from CH_2I_2.

Since all fragment oscillations share a common frequency, we postulate that the modulations are a result of wave packet motion in a single electronic state. As for which state is responsible, we can rule out the electronic ground state of the neutral molecule for two reasons. First, the modulation frequency does not match any of the measured normal mode frequencies nor any differences between normal mode frequencies in this state (Table II lists the relevant ground state modes). Second, it is very unlikely that a large amplitude vibrational wave packet would be formed in the ground electronic state of the molecule through nonresonant excitation. Furthermore, the anticorrelation (π relative phase) between the CH_2I^+ and $CH_2I_2^+$ yields suggests that the

Downloaded 06 Dec 2007 to 129.49.60.83. Redistribution subject to AIP license or copyright; see http://jcp.aip.org/jcp/copyright.jsp

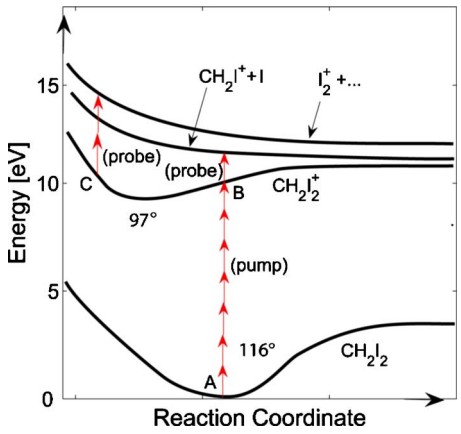

FIG. 3. (Color online) Cartoon of the involved potential energy surfaces. The pump pulse lifts the molecule from point A to an intermediate state ($CH_2I_2^+$ in this diagram) that is shifted along the reaction coordinate relative to the ground state. This launches a wave packet that oscillates between its outer (B) and inner (C) turning points. At point B, the absorption of one photon from the probe pulse can lift this wave packet to a dissociative level leading to CH_2I^+. At point C, excitation by the probe pulse leads to dissociation with I_2^+ as a product.

CH_2I^+ is being formed by lifting a wave packet from a bound state of $CH_2I_2^+$ to a dissociative state which leads to the production of CH_2I^+. Therefore, we propose the process that can be described by

$$CH_2I_2(X) \xrightarrow{\text{pump}} CH_2I_2^+ \xrightarrow{\text{probe}} I_2^+ + \cdots, \quad (1)$$

$$\xrightarrow{\text{probe}} CH_2I^+ + I, \quad (2)$$

where the intermediate step of $CH_2I_2^+$ corresponds to a low-lying electronic state of the molecular ion.

Figure 3 shows a cartoon of the relevant potentials. The choice of reaction coordinate and equilibrium points is motivated by the structure of the ion relative to the neutral molecule, as discussed below. A vibrational wave packet is launched in the molecular ion through multiphoton ionization. The subsequent elimination of CH_2I^+ and I_2^+ is driven by the probe pulse lifting the vibrational wave packet from the potential corresponding to the molecular ion ($CH_2I_2^+$) into two different dissociative states, where the timing of the probe pulse controls which product is favored. The modulation in the parent ion yield is due to the depopulation of the wave packet in the ground ionic state.

The modulation at 111 cm^{-1} in each fragment ion yield has a well-defined phase relative to zero pump-probe time delay. The phases of the modulations in the $CH_2I_2^+$ and I_2^+ yields relative to zero pump-probe delay are π (i.e., minimum yield at $t=0$), while the phase of the modulation in the CH_2I^+ yield is 0 (i.e., maximum yield at $t=0$). The fact that CH_2I^+ and I_2^+ oscillate out of phase (π phase difference) indicates that the positions for optimal production of CH_2I^+ and I_2^+ have to be close to the inner and outer turning points (B and C) of the potential. Furthermore, since the phase of the CH_2I^+ modulation is 0 relative to zero pump-probe delay (i.e., CH_2I^+ emission has its maximum at time zero), the position along the reaction coordinate for optimal branching to CH_2I^+ [point (B)] must happen at the same position as the ground state minimum [point (A)]. One might wonder why the phases of the I_2^+ and $CH_2I_2^+$ signals are the same if I_2^+ is formed at the expense of $CH_2I_2^+$. Table I shows that the amplitudes of the oscillations in the CH_2I^+ and $CH_2I_2^+$ signals are comparable to each other but much larger than in I_2^+. The maximal I_2^+ elimination takes place close to minimal CH_2I^+ production, which is again close to point C. Thus, the modulation in $CH_2I_2^+$ is dominated by the formation of CH_2I^+ rather than I_2^+, which is why the I_2^+ and $CH_2I_2^+$ yields are correlated.

While our observations are consistent with the wave packet dynamics taking place in the molecular ion, an earlier work has focused on highly excited neutral states. In particular, formation of I_2 with radiation of between 9.3 and 10.2 eV has been associated with excitation to Rydberg states and a C–I σ^* antibonding state.[22] The recurrent wave packet signal and production of $CH_2I_2^+$ in our measurements indicate that the intermediate state is nondissociative. The fact that our I_2^+ yield is an order of magnitude greater than those reported from neutral states suggests that our I_2^+ signal is not derived from excitation of a highly excited neutral (Rydberg) state. Furthermore, the presence of molecular ions at zero probe pulse intensity means that the ionization is definitely taking place during the pump pulse, and the modulations we observe match the I–C–I scissors frequency calculated for the molecular ion (shown in Table II).

The structure of the molecular ion is consistent with the wave packet dynamics occurring in a low-lying ionic state. The I–C–I angle is 97° in the ionic state,[25] whereas the I–C–I angle for the neutral ground state is 116°.[26] Thus, ionization of the molecule can launch a large amplitude "bending wave packet" that moves initially from a larger angle to a smaller one, consistent with the π phase of the I_2^+ modulation. At the inner turning point, both iodine atoms are close and tend to form an iodine molecule, while at the outer turning point, they tend to dissociate separately to form CH_2I^+ and I. The agreement between our measured oscillation frequency and the calculated I–C–I bending frequency, in conjunction with the equilibrium angles for the neutral and ion, motivate the structure of Fig. 3.

Finally, Fig. 2 shows that the 111 cm^{-1} oscillations appear at different probe pulse intensities for different ions. The CH_2I^+ (and, consequently, the $CH_2I_2^+$ as well) oscillations start as soon as the the probe pulse intensity is nonzero, indicating that the transition from $CH_2I_2^+$ to CH_2I^+ is linear in probe pulse intensity and, therefore, driven by single photon absorption. Since the I_2^+ modulation does not initially increase linearly with probe intensity, the formation of I_2^+ from $CH_2I_2^+$ is a nonlinear process and requires the absorption of at least two photons.

Our measurements lead to a simple and intuitive picture of the dynamics leading to the formation of I_2^+. The pump pulse ionizes the CH_2I_2 molecule, launching a vibrational wave packet in a low-lying ionic state. This wave packet has a significant displacement along the I–C–I bend coordinate since the equilibrium angle for the ion is smaller than for the neutral. This bending motion modulates the amounts of I_2^+ and CH_2I^+ formed by the probe pulse, with smaller I–C–I angles favoring I_2^+ production and larger I–C–I angles favor-

Downloaded 06 Dec 2007 to 129.49.60.83. Redistribution subject to AIP license or copyright; see http://jcp.aip.org/jcp/copyright.jsp

ing CH_2I^+ formation. It has been argued that I–C–I bending motion should influence I_2 production for a synchronous concerted elimination process, and our measurements are consistent with this intuitive argument. In fact, vibrational coherences have been observed earlier in the I_2 product.[18] In this work, we observe modulations in the concerted elimination yield driven by vibrational coherences in the reactant molecule.

While it is natural that the bending motion along the I–C–I coordinate influences the formation of I_2^+, this is clearly not the only dynamics affecting the production of I_2^+. Immediately following zero time delay, the $CH_2I_2^+$ and I_2^+ signals drop dramatically, while the CH_2I^+ signal increases commensurately. We believe that these large changes are a result of coupling between two low lying ionic potentials or motion along the C–I stretching coordinates, such that the wave packet will not return to its original position and shape on the excited PES.[29] The analysis of this motion will be the subject of a forthcoming publication.

V. CONCLUSION

In conclusion, we have studied the influence of vibrational wave packet motion on the formation of I_2^+ (via concerted elimination) and CH_2I^+ from CH_2I_2 through a series of pump-probe measurements. Our measurements are consistent with a simple picture of the dynamics, where bending motion along the I–C–I coordinate in the molecular ion leads to a modulation in both yields as a function of pump-probe delay. The formation of I_2^+ is largest when the wave packet is at the minimum I–C–I angle, while the formation of CH_2I^+ is largest when the wave packet reaches the maximum I–C–I angle during each period of vibration. We are currently expanding our analysis to include motion along other coordinates of the molecular ion and to model the wave packet dynamics in a two-dimensional potential energy surface calculated by *ab initio* molecular structure calculations.

ACKNOWLEDGMENTS

We are grateful to James Marecek from the Chemical Synthesis Center at Stony Brook University for supplying the CH_2I_2 used in our experiments and to Tamas Rozgonyi for helpful discussions. Dominik Geißler acknowledges support from the Studienstiftung des Deutschen Volkes. We gratefully acknowledge support from the National Science Foundation under Award No. 0555214.

[1] Z. Amitay, J. Ballard, H. Stauffer, and S. Leone, Chem. Phys. **267**, 141 (2001).
[2] E. Skovsen, M. Machholm, T. Ejdrup, J. Thogersen, and H. Stapelfeldt, Phys. Rev. Lett. **89**, 133004 (2002).
[3] J. Itatani, J. Levesque, D. Zeidler, H. Niikura, H. Pepin, J. C. Kieffer, P. B. Corkum, and D. M. Villeneuve, Nature (London) **432**, 867 (2004).
[4] B. J. Sussman, D. Townsend, M. Y. Ivanov, and A. Stolow, Science **314**, 278 (2006).
[5] A. H. Zewail, Phys. Today **33**(11), 27 (1980).
[6] T. Baumert, B. Bühler, R. Thalweiser, and G. Gerber, Phys. Rev. Lett. **64**, 733 (1990).
[7] T. Baumert, C. Röttgermann, C. Rothenfusser, R. Thalweiser, V. Weiss, and G. Gerber, Phys. Rev. Lett. **69**, 1512 (1992).
[8] Š. Vajda, A. Bartelt, E.-C. Kaposta, T. Leisner, C. Lupulescu, S. Minemoto, P. Rosendo-Francisco, and L. Wöste, Chem. Phys. **267**, 231 (2001).
[9] R. A. Bartels, T. C. Weinacht, S. R. Leone, H. C. Kapteyn, and M. M. Murnane, Phys. Rev. Lett. **88**, 033001 (2002).
[10] J. Hauer, H. Skenderovic, K. L. Kompa, and M. Motzkus, Chem. Phys. Lett. **421**, 523 (2006).
[11] T. Rozgonyi and L. González, J. Phys. Chem. A **106**, 11150 (2002).
[12] N. H. Damrauer, C. Dietl, G. Krampert, S.-H. Lee, K.-H. Jung, and G. Gerber, Eur. Phys. J. D **20**, 71 (2002).
[13] *Chemistry and Radiation Changes in the Ozone Layer* (Kluwer, Dordrecht, 2001).
[14] D. G. Abrashkevich, M. Shapiro, and P. Brumer, J. Chem. Phys. **116**, 5584 (2002).
[15] W. Radloff, P. Farmanara, V. Stert, E. Schreiber, and J. Huber, Chem. Phys. Lett. **291**, 173 (1998).
[16] Q. Zhang, U. Marvet, and M. Dantus, Faraday Discuss. **108**, 63 (1997).
[17] Z.-H. Liu, Y.-Q. Wang, J.-J. Ma, L. Wang, and G.-Z. He, Chem. Phys. Lett. **383**, 198 (2004).
[18] U. Marvet and M. Dantus, Chem. Phys. Lett. **256**, 57 (1996).
[19] I. Pastirk, E. J. Brown, Q. Zhang, and M. Dantus, J. Chem. Phys. **108**, 4375 (1998).
[20] F. Langhojer, D. Cardoza, M. Baertschy, and T. Weinacht, J. Chem. Phys. **122**, 014102 (2005).
[21] M. A. Dugan, J. X. Tull, and W. S. Warren, J. Opt. Soc. Am. B **14**, 2348 (1997).
[22] H. Okabe, M. Kawasaki, and Y. Tanaka, J. Chem. Phys. **73**, 6162 (1980).
[23] S. M. Hankin, D. M. Villeneuve, P. B. Corkum, and D. M. Rayner, Phys. Rev. A **64**, 013405 (2001).
[24] L. Fang and G. N. Gibson, Phys. Rev. A **75**, 063410 (2007).
[25] X. Zheng and D. L. Phillips, J. Phys. Chem. A **104**, 6880 (2000).
[26] D. L. Phillips and W.-H. Fang, J. Org. Chem. **66**, 5890 (2001).
[27] M. M. Heckscher, L. Sheps, D. Bingemann, and F. F. Crim, J. Chem. Phys. **117**, 8917 (2002).
[28] W. M. Kwok and D. L. Phillips, J. Chem. Phys. **104**, 2529 (1996).
[29] J. Zhang, E. Heller, D. Huber, D. Imre, and D. Tannor, J. Chem. Phys. **89**, 3602 (1988).

Downloaded 06 Dec 2007 to 129.49.60.83. Redistribution subject to AIP license or copyright; see http://jcp.aip.org/jcp/copyright.jsp